Organic LETTERS

Letter

pubs.acs.org/OrgLett

Strongly Dichroic Organic Films via Controlled Assembly of Modular Aromatic Charge-Transfer Liquid Crystals

Ariana Gray Bé, Cheryl Tran, Riley Sechrist, and Joseph J. Reczek*

The Department of Chemistry and Biochemistry, Denison University, 500 West Loop, Granville, Ohio 43023, United States

Supporting Information

ABSTRACT: The formation of highly anisotropic organic thin films based on the designed self-assembly of mixed-stack liquid crystals is reported. A series of alkoxyanthracene donors is combined in a modular fashion with a naphthalenediimide acceptor to generate new charge-transfer columnar liquid crystals. Materials characterization and molecular modeling provides insight into structure−function relationships in these organic materials that lead to the striking bulk dichroic properties of certain molecular assemblies.

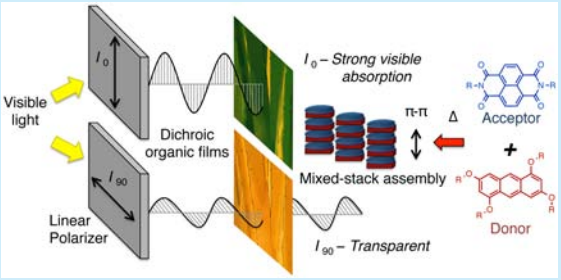

Control over the molecular alignment of organic liquid crystals, resulting in functional anisotropic properties, has led to their ubiquitous use in technologies.[1] Development of new organic materials offers potential advantages in cost, processing, and lightweight functionality for a wide range of applications.[2] Strategies in supramolecular chemistry, particularly directed noncovalent interactions, offer creative approaches for designing the ordered self-assembly of organic materials having anisotropic features required of many functional applications.[3]

Aromatic donor−acceptor or charge-transfer (CT) interactions are directed $\pi-\pi$ interactions that have often been used to achieve elegant control of molecular structure in solution.[4] Related bulk-phase materials consisting of alternating electron-rich and electron-poor aromatics are currently enjoying a renaissance in organic materials research.[5,6] These mixtures often exhibit CT absorption properties distinct from those of the component molecules due to the direct excitation of the $\text{donor}_{\text{HOMO}}$ to $\text{acceptor}_{\text{LUMO}}$ in $\pi-\pi$-stacked components (Figure 1a,b). Recent reports highlight emerging anisotropic properties of CT cocrystals relevant to developing functional organic materials, including polarized absorption and emission of light,[7] ambipolar charge mobility,[8] photoconductivity,[9] and ferroelectric behavior.[10] However, these crystalline systems require complex design elements beyond donor−acceptor interactions to achieve highly ordered materials, and stable film formation and processing is extremely challenging.[7−11] It is therefore highly attractive to develop CT liquid crystalline systems with the anisotropic properties of CT cocrystals. Inspired in part by early work from Ringsdorf and co-workers,[12] examples of CT liquid crystals, termed donor−acceptor columnar liquid crystals (DACLC), have been reported.[13] However, anisotropic properties in this fascinating class of materials remains unexplored and undeveloped.

Here, we report the formation of several new DACLC materials based on the straightforward 1:1 combination of *n*-alkoxyanthracene donors (**1**−**4**) with a naphthalenediimide acceptor **5** (Figure 1c). All mixtures exhibit mesophase behavior and new CT absorbance in the visible spectrum. Of particular interest, DACLC materials incorporating tetrasubstituted donors **3a**−**d** were found to yield thin films with well-ordered structures with strong dichroic properties. This was not observed in the other mixtures in this study. Structure−property relationships in these materials related to the ordered anisotropy of certain DACLC films are investigated. To the best of our knowledge, the DACLCs presented here are unprecedented in their dichroic absorption properties as bulk

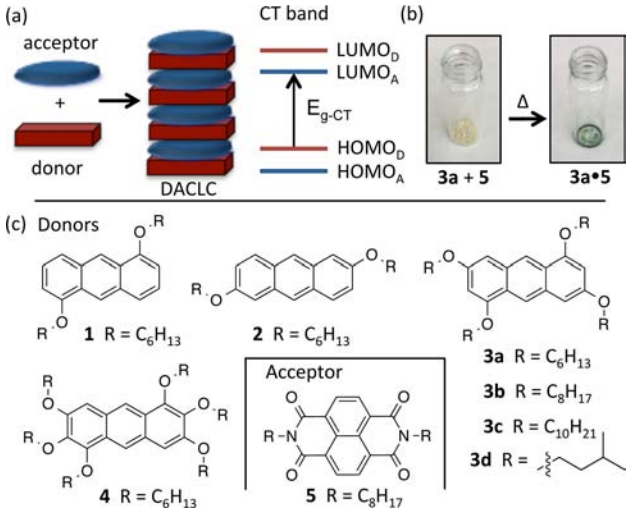

Figure 1. (a) Schematic of mixed-stack DACLCs and CT absorption. (b) Representative bulk color change of mixtures upon melting. (c) Donors and acceptors used in this study.

Received: August 19, 2015
Published: September 16, 2015

DOI: 10.1021/acs.orglett.5b02399
Org. Lett. 2015, 17, 4834−4837

organic small molecule films containing no directing dye component. This work illustrates the ability to design anisotropic properties of stable CT liquid−crystalline films using only supramolecular aromatic donor−acceptor interactions.

The UV/vis spectra of all DACLCs investigated show a significant CT band in the visible spectrum, clearly evident in bulk samples as a dramatic color change on initial melting of each mixture (Figure 1b). This is attributed to the direct excitation of electrons from donor$_{HOMO}$ to acceptor$_{LUMO}$ in neighboring $\pi-\pi$ stacked components (Figure 1a). Consistent with previous studies, DFT calculations on component molecules accurately predict the onset of absorption in these mixed-stack materials.[14] Comparing mixtures made with anthracene donors **1**−**4**, there is substantial variation in the intensity of absorption at $\lambda_{max\text{-}CT}$ (ε_{CT}) (Figure 2a).

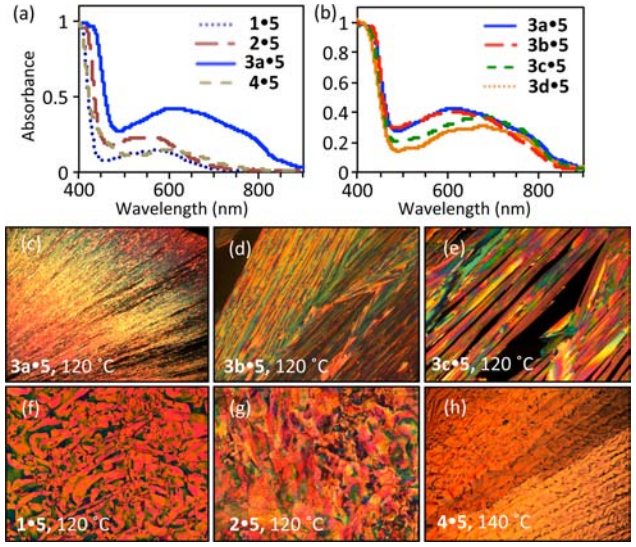

Figure 2. Normalized thin-film UV/vis absorption spectra taken in the first mesophase of (a) **1·5**, **2·5**, **3a·5**, **4·5**; (b) **3a·5**, **3b·5**, **3c·5**, and **3d·5**. (c−h) Representative polarized optical microscopy images of initial mesophases under cross polarized light at 40× magnification.

Interestingly, mixture **3a·5** exhibited an ε_{CT} significantly greater than mixtures with donors **1**, **2**, and **4**. This intense CT absorption persists on altering the side chain, illustrating that core geometry largely dictates this property (Figure 2b).

The phase behavior of DACLCs was characterized using differential scanning calorimetry (DSC) and polarized optical microscopy (POM). All mixtures exhibited at least two phase transitions distinct from those of the component molecules (Table S2, Supporting Information). Mixtures **3a·5**, **3b·5**, and **3c·5** have initial transitions that are remarkably similar in both energy and temperature suggesting commonality in the structure of their respective mesophases. Thin film samples of mesophase materials were formed by sandwiching ∼1 mg of material between cleaned glass coverslips, heating, and then cooling at 1°/min from the isotropic melt. Comparing the optical textures of these mixtures further supports the similarity of their initial mesophases (Figure 2c,d,e). In each mixture the phase grows from the isotropic liquid as narrow, colorful structures that propagate linearly over areas on the order of 1 cm^2. The moderate phase transition energy and flat, long-range linear texture observed for these DACLCs suggests a 2-D ordered columnar Col$_L$ phase. On cooling to the second phase transition, each of the **3x·5** series materials maintains this overall structure, the only visible change being an apparent widening of the linear formations. Mesophase samples all have fluid character, passing a slip test in both the first and second mesophase. Of these materials, only **3b·5** transitions to a crystalline state on further cooling, evidenced by the loss of any fluid character. In contrast, mixture **1·5** shows a *schlieren* texture consistent with a columnar nematic phase (N_{Col}), and the high-energy amorphous transition of **2·5** indicates direct formation of a Col$_p$ phase (Figure 2f,g). Upon further cooling, both **1·5** and **2·5** crystallize with a coinciding loss of color, emphasizing the unpredictable effect of crystal packing forces on CT properties.[15] The low energy initial transition of mixture **4·5** yields thin reticular structures indicative of a Col$_r$ phase (Figure 2h). This mixture also loses its CT absorption on phase transition, likely due to the steric interactions of the adjacent substituents, which perturb stacking.

Viewing DACLC films with linearly polarized light (LPL) illustrates the impressive ordered anisotropy of the Col$_L$ phase materials (Figure 3a−f). When the transmission vector (I) of

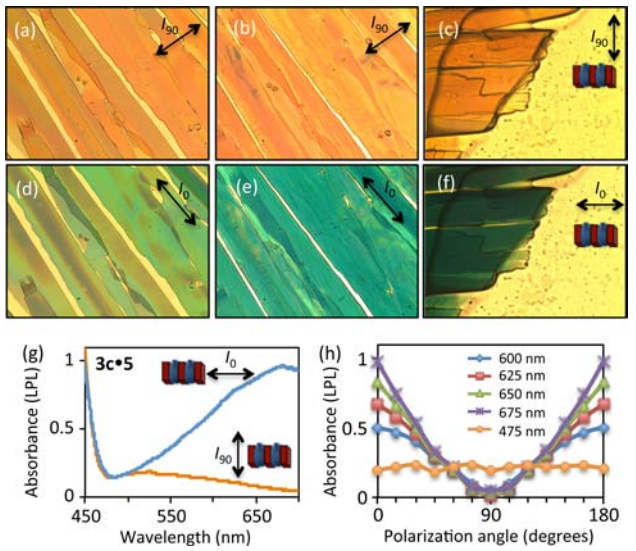

Figure 3. LPL microscopy with I oriented perpendicular (a−c) and parallel (d−f) to the propagation direction of the films, 200× magnification. (a, d) **3b·5**, 100 °C; (b, e) **3b·5**, 70 °C; (c, f) **3a·5**, 120 °C. (g) Normalized LPL absorption spectra of **3c·5** with polarization aligned parallel and perpendicular to the long-axis of the film. (h) Absorption of **3c·5** at specified wavelengths on rotation of a single polarizer.

the LPL is directed perpendicular to the long-axis of the Col$_L$ film structures (I_{90}), the films appear off-white/pale yellow. On rotating the polarizer 90° to align I parallel to the film structures (I_0), a dramatic change of color to a dark blue-green is observed. All of the **3x·5** mixtures exhibit this stark dichroic behavior. Viewing the advancing edge of the films reveals the sheet-like layers of the Col$_L$ phase; thin layers of the material can be seen growing from the isotropic liquid with the formation of several layers (Figure 3c,f). As these DACLCs transition to the Col$_p$ phase the strong anisotropy persists and is present at room temperature in **3a·5** and **3c·5**.

The intense dichroic absorption in these materials results from a directional dependence of CT absorption in the highly ordered aromatic donor−acceptor stacks. Polarized UV/vis spectroscopy of the Col$_L$ phase shows a strong CT band when

DOI: 10.1021/acs.orglett.5b02399
Org. Lett. 2015, 17, 4834−4837

incident light is oriented at I_0 and a complete lack of CT absorption at I_{90} (Figure 3g). Measurement of λ_{CT} at 5° intervals of I confirms a maximum and minimum ε_{CT} at I_0 and I_{90}, respectively, with a dichroic ratio >30 for combinations of all compounds **3a–d** with **5** at their respective $\lambda_{max\text{-}CT}$ (as illustrated for **3c·5** in Figure 3h). This is in contrast to absorbance at 475 nm, which has no CT component and shows no dependence on I. As direct excitation of the donor$_{HOMO}$ to acceptor$_{LUMO}$ can only occur if the transmitting light has a vector component in the stacking direction, these results unambiguously establish that the direction of donor–acceptor stacking is perfectly parallel to the long axis of the Col$_L$ structures. No dependence of CT absorption on I was observed for DACLCs **1·5**, **2·5**, or **4·5**.

Phase structures of DACLC **3b·5** were investigated using variable-temperature powder-XRD to gain insight into the distinctive molecular assembly leading to dichroic films (Figure 4; Table S3 in Supporting Information). In the Col$_L$ phase, only

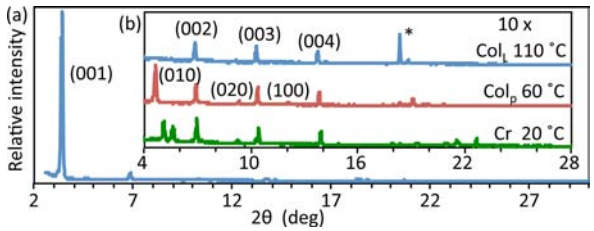

Figure 4. (a) X-ray diffraction data of the Col$_L$ phase of **3b·5** at 110 °C. (b) Magnified X-ray diffraction data of the phases of **3b·5** at 110, 60, and 20 °C. *The sharp peak at 2θ = 18.35 is an artifact of the sample holder; it is identical in position and intensity/scan at all temperatures.

five discrete peaks are observed, all relating to the (001) Bragg reflection in a ratio of 1:2:3:4:6. Broad peaks are also observed at a d spacing of ~12.5 Å due to the alkyl chain halo and at ~7.3 Å corresponding to the π–π–π spacing of the donor–acceptor–donor mixed stack. The broad 7.3 Å peak represents the (100) reflection, establishing the 2-D order of the Col$_L$ phase. On cooling, the (001) reflections are maintained, and two new sharp peaks are observed at 19.1 and 9.5 Å at a 1:2 ratio, corresponding to the (010) index. This phase also exhibits sharpening of the (100) peak at 7.3 Å but maintains the alkyl halo and lack of additional large-angle reflections consistent with 3-D order in a Col$_P$ phase. On crystallization the (010) index shifts and is divided into two new peaks, and the (100) index is no longer observed. This supports adoption of a new donor–acceptor stacking orientation, consistent with the observed change in CT absorption.

Geometry optimization was performed at the DFT 6-31G* level on components and donor–acceptor dimers to gain insight into the relative orientation of the **3x·5** donor–acceptor cores in the anisotropic films (Figure 5). The electrostatic potential of components are well matched, and calculations yield a face-centered geometry with a donor–acceptor π–π distance of 3.6 Å (±0.15 Å) with a significant dipole of 2.08 debye for the **3x·5** dimer (Figure 5a,b). The optimized torsional position places alkyl chains at a reasonable distance and appears to be dominated by electrostatic interactions between the oxygens at the 1,5 positions of the donor with the electropositive hydrogens of the NDI core. This suggests self-assembly of the alternating mixed-stack columns is governed by the complementary electrostatic potential of the aromatic surfaces, while the positional orientation of stacked aromatics is dominated by electrostatic interactions between concentrated areas of electron density on core substituents.[16,17]

Interestingly, orbital overlap between the donor$_{HOMO}$ and acceptor$_{LUMO}$ is nearly optimized at the calculated torsional orientation for the **3x·5** cores (Figure 5c). Compared to mixed stacks with donors **1** and **2**, there is significantly less freedom of rotation for **3x** donors to rotate within a column relative to the NDI acceptor due to the four alkyl substituents (Figure 5b,d). This structural element likely leads to increased orbital overlap, on average, for the **3x·5** series. Better orbital overlap will increase the likelihood of productive photon absorption and may explain the relatively intense CT absorbance observed for the **3x·5** materials compared to that of **1·5** and **2·5**.

The intercolumnar assembly and phase structure of **3b·5** was further modeled using the minimized stacking geometry and van der Waals radii of the **3b·5** alkyl chains, informed by the powder-XRD data. The resulting molecular arrangement fits remarkably well with the measured d spacing of reflections, corresponding to an a, b, c lattice geometry of 7.3, 19.6, and 25.6 Å (Figure 5e). The (001) spacing of 25.6 Å represents the full "width" of a donor–acceptor complex. This packing geometry would result in the high intensity of the (001) peak

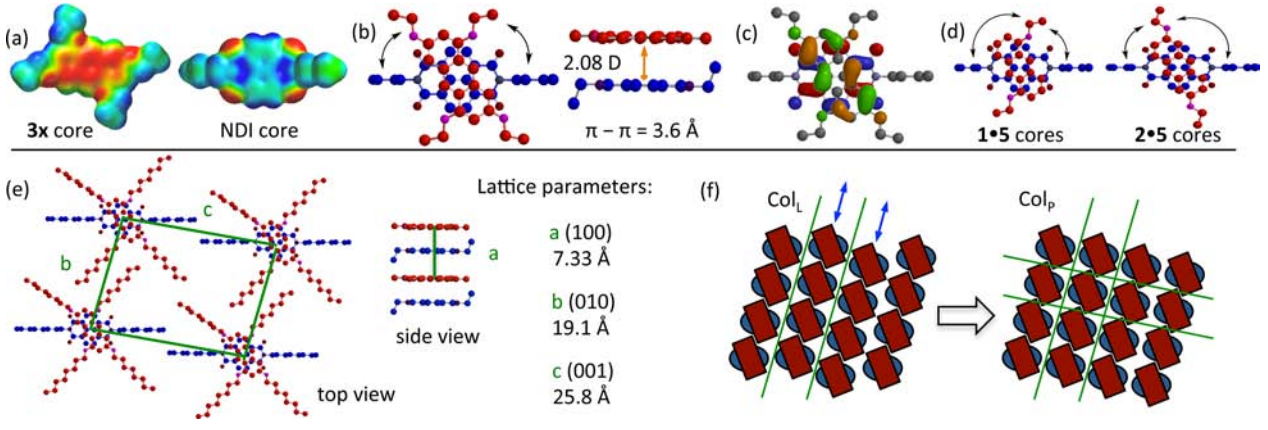

Figure 5. Modeling of **3x** anthracene and NDI cores (B3LYP functional with 6-31G*; Spartan 14 Mac): (a) electrostatic surface potential; (b) top and side view of optimized stacking orientation; (c) donor$_{HOMO}$–acceptor$_{LUMO}$ overlap; (d) relative rotational flexibility of the **1·5** and **2·5** cores; (e) packing geometry modeled on optimization and powder-XRD data; (f) representation of Col$_L$ and Col$_P$ phases.

DOI: 10.1021/acs.orglett.5b02399
Org. Lett. 2015, 17, 4834–4837

and is consistent with a 2-D Col_L phase in which rows of mixed-stack columns form lamellar sheets that have some freedom to slide with respect to each other (Figure 5e). Upon transition to the Col_p phase, the lamellar degree of freedom is frozen, leading to observation of the (010) reflection, while the overall structure and anisotropic properties of the donor−acceptor stacks are maintained. This model suggests that the combination of substituent positioning and relatively restricted torsional movement between neighboring molecules leads to the stable, highly ordered structure seen only in the **3x·5** series.

The remarkable dichroic behavior of the **3x·5** series illustrates unprecedented supramolecular control over long-range anisotropic properties in bulk films of organic CT liquid crystalline materials. The tetrasubstitution pattern of the **3x** anthracene core yields an electrostatic surface that is well matched to the NDI acceptor while limiting orientational freedom of the CT stacking geometry. These structural features lead to formation of a Col_L phase with highly ordered mixed stacks directed along the long axis of film morphology. An intense CT band is only observed on illumination with light having a transmission vector parallel to the stacking direction; films are almost completely transparent to visible LPL oriented in the orthogonal direction. These features are maintained on transition to a Col_p phase and present at room temperature in two organic materials. Work is currently underway exploring these structure/function relationships further, as well as investigation of additional anisotropic properties and control over bulk alignment of these stable organic CT mesophases.

■ ASSOCIATED CONTENT

Supporting Information

The Supporting Information is available free of charge on the ACS Publications website at DOI: 10.1021/acs.orglett.5b02399.

Experimental details including synthesis, spectroscopic data, and additional data (PDF)

■ AUTHOR INFORMATION

Corresponding Author

*E-mail: reczekj@denison.edu.

Notes

The authors declare no competing financial interest.

■ ACKNOWLEDGMENTS

We thank Loryn Holokai and Margo MacDonald (Denison University) for aid with synthesis, Jordan Fantini (Denison University) and Rebecca Reczek (Ohio State University) for helpful discussions, and the Denison University R. C. Good Faculty Fellowship for J.J.R. sabbatical support. This work was supported in part by grants from the National Science Foundation (CHE-1152965 and 1040302).

■ REFERENCES

(1) (a) Lee, S. H.; Bhattacharyya, S. S.; Jin, H. S.; Jeong, K.-U. *J. Mater. Chem.* **2012**, *22*, 11893. (b) Kim, K.-H.; Song, J.-K. *NPG Asia Mater.* **2009**, *1*, 29.

(2) (a) Stoppa, M.; Chiolerio, A. *Sensors* **2014**, *14*, 11957. (b) Anthony, J. E. *Nat. Mater.* **2014**, *13*, 773. (c) Coskun, A.; Spruell, J. M.; Barin, G.; Dichtel, W. R.; Flood, A. H.; Botros, Y. Y.; Stoddart, J. F. *Chem. Soc. Rev.* **2012**, *41*, 4827.

(3) (a) Stupp, S. I.; Palmer, L. C. *Chem. Mater.* **2014**, *26*, 507. (b) Zhou, J.; Du, X.; Gao, Y.; Shi, J.; Xu, B. *J. Am. Chem. Soc.* **2014**, *136*, 2970. (c) *Supramolecular Soft Matter*; Nakanishi, T., Ed.; John Wiley & Sons; Hoboken, 2011. (d) Hoogboom, J.; Swager, T. M. *J. Am. Chem. Soc.* **2006**, *128*, 15058. (e) Pisula, W.; Kastler, M.; Wasserfallen, D.; Robertson, J. W. F.; Nolde, F.; Kohl, C.; Müllen, K. *Angew. Chem., Int. Ed.* **2006**, *45*, 819.

(4) For recent reviews, see: (a) Das, A.; Ghosh, S. *Angew. Chem., Int. Ed.* **2014**, *53*, 2038. (b) Barin, G.; Coskun, A.; Fouda, M. M. G.; Stoddart, J. F. *ChemPlusChem* **2012**, *77*, 159. (c) Klosterman, J. K.; Yamauchi, Y.; Fujita, M. *Chem. Soc. Rev.* **2009**, *38*, 1714.

(5) (a) Yamada, J.-I.; Akutsu, H. *Chem. Rev.* **2004**, *104*, 5057. (b) Praefcke, K.; Singer, D. In *Handbook of Liquid Crystals*; Demus, D., Goodby, J., Gary, G. W., Spiess, H.-W., Vill, V., Eds.; Wiley-VCH: Weinheim, 1998; Vol. *2B*, pp 945−967. (d) Soos, Z. G. *Annu. Rev. Phys. Chem.* **1974**, *25*, 121. (e) Patrick, C. R.; Prosser, G. S. *Nature* **1960**, *187*, 1021.

(6) (a) Tayi, A. S.; Kaeser, A.; Matsumoto, M.; Aida, T.; Stupp, S. I. *Nat. Chem.* **2015**, *7*, 281. (b) Qin, W.; Xu, B.; Ren, S. *Nanoscale* **2015**, *7*, 9122. (c) Goetz, K. P.; Vermeulen, D.; Payne, E.; Kloc, C.; McNeil, L. E.; Jurchescu, O. D. *J. Mater. Chem. C* **2014**, *2*, 3065. (d) Kumar, M.; Rao, K. V.; George, S. J. *Phys. Chem. Chem. Phys.* **2014**, *16*, 1300.

(7) Zhu, W.; Zheng, R.; Fu, X.; Fu, H.; Shi, Q.; Zhen, Y.; Dong, H.; Hu, W. *Angew. Chem., Int. Ed.* **2015**, *54*, 6785.

(8) (a) Geng, H.; Zheng, X.; Shuai, Z.; Zhu, L.; Yi, Y. *Adv. Mater.* **2015**, *27*, 1443. (b) Su, Y.; Li, Y.; Liu, J.; Xing, R.; Han, Y. *Nanoscale* **2015**, *7*, 1944. (c) Zhu, L.; Yi, Y.; Li, Y.; Kim, E.-G.; Coropceanu, V.; Brédas, J.-L. *J. Am. Chem. Soc.* **2012**, *134*, 2340.

(9) Yu, W.; Wang, X.-Y.; Li, J.; Li, Z.-T.; Yan, Y.-K.; Wang, W.; Pei, J. *Chem. Commun.* **2013**, *49*, 54.

(10) Tayi, A. S.; Shveyd, A. K.; Sue, A. C.-H.; Szarko, J. M.; Rolczynski, B. S.; Cao, D.; Kennedy, T. J.; Sarjeant, A. A.; Stern, C. L.; Paxton, W. F.; Wu, W.; Dey, S. K.; Fahrenbach, A. C.; Guest, J. R.; Mohseni, H.; Chen, L. X.; Wang, K. L.; Stoddart, J. F.; Stupp, S. I. *Nature* **2012**, *488*, 485.

(11) (a) Blackburn, A. K.; Sue, A. C. H.; Shveyd, A. K.; Cao, D.; Tayi, A.; Narayanan, A.; Rolczynski, B. S.; Szarko, J. M.; Bozdemir, O. A.; Wakabayashi, R.; Lehrman, J. A.; Kahr, B.; Chen, L. X.; Nassar, M. S.; Stupp, S. I.; Stoddart, J. F. *J. Am. Chem. Soc.* **2014**, *136*, 17224. (b) Kumar, M.; George, S. J. *Chem. - Asian J.* **2014**, *9*, 2427. (c) Peebles, C.; Alvey, P. M.; Lynch, V.; Iverson, B. L. *Cryst. Growth Des.* **2014**, *14*, 290.

(12) (a) Ringsdorf, H.; Ebert, M.; Karthaus, O.; Kohne, B.; Praefcke, K.; Wendorff, J.; Wüsterfeld, R.; Bengs, H. *Adv. Mater.* **1990**, *2*, 141. (b) Ringsdorf, H.; Wustefeld, R.; Zerta, E.; Ebert, M.; Wendorff, J. H. *Angew. Chem., Int. Ed. Engl.* **1989**, *28*, 914.

(13) (a) Wang, J.-Y; Yan, J.; Ding, L.; Ma, Y.; Pei, J. *Adv. Funct. Mater.* **2009**, *19*, 1746. (b) Reczek, J. J.; Villazor, K. R.; Lynch, V.; Swager, T. M.; Iverson, B. L. *J. Am. Chem. Soc.* **2006**, *128*, 7995. (c) Park, L. Y.; Hamilton, D. G.; McGehee, E. A.; McMenimen, K. A. *J. Am. Chem. Soc.* **2003**, *125*, 10586.

(14) Leight, K. R.; Esarey, B. E.; Murray, A. E.; Reczek, J. *Chem. Mater.* **2012**, *24*, 3318.

(15) Alvey, P. M.; Reczek, J. J.; Lynch, V.; Iverson, B. L. *J. Org. Chem.* **2010**, *75*, 7682.

(16) Hunter, C. A.; Sanders, J. K. M. *J. Am. Chem. Soc.* **1990**, *112*, 5525.

(17) (a) Parrish, R. M.; Sherrill, C. D. *J. Am. Chem. Soc.* **2014**, *136*, 17386. (b) Wheeler, S. E. *Acc. Chem. Res.* **2013**, *46*, 1029.

DOI: 10.1021/acs.orglett.5b02399
Org. Lett. 2015, 17, 4834−4837